

A TRIANGULATION METHOD FOR 3D-MEASUREMENT OF SPECULAR SURFACES

R. Muhr^{a,*}, G. Schutte^a, M. Vincze^b

^a Infineon Technologies Austria AG, 9500 Villach, Austria - (Robert.Muhr, Gerrit.Schutte)@infineon.com

^b Vienna University of Technology, ACIN - Automation and Control Institute, Gusshausstrasse 27-29 / E376,
1040 Vienna, Austria – vincze@acin.tuwien.ac.at

Commission V, WG V/1

KEY WORDS: Metrology, Calibration, Measurement, Reconstruction, Triangulation, Surface, Three-dimensional, Close Range

ABSTRACT:

In this paper we present a method for finding absolute 3D-coordinates of surface points on specular objects. We make use of a deflectometric measurement system consisting of a camera and a LC display and modify the measurement setup with a wire. The wire defines a straight line in object space and therefore allows us to constrain the direction of some rays reflected on the surface. For those rays an object point can be computed by a triangulation between the camera ray and the reflected camera ray. The measured points can be used as starting values for a region-growing approach, in order to reconstruct smooth specular surfaces.

In diesem Beitrag zeigen wir eine Methode mit welcher auf spiegelnden Objekten absolute 3D-Objektkoordinaten bestimmt werden können. Wir verwenden ein deflektometrisches Meßsystem und modifizieren dieses mit einem Draht. Mit dem Draht legen wir eine Raumgerade fest, welche es uns ermöglicht für die Bestimmung der Raumlage einiger reflektierter Kamerasichtstrahlen einen zusätzlichen Freiheitsgrad zu beschränken. Dadurch kann für diese Sichtstrahlen durch eine Triangulation zwischen dem Kamerasichtstrahl und dem reflektierten Sichtstrahl ein Objektpunkt berechnet werden. Die mit dieser Methode bestimmten Punkte können als Startwerte für ein Regionenwachstum-Verfahren verwendet werden, um so stetige Oberflächen von spiegelnden Objekten zu rekonstruieren.

1. INTRODUCTION

Classical image-based methods like photometric stereo, shape from shading and light section triangulation are widely used for the measurement of diffuse reflecting surfaces. These methods all require that the surfaces of the objects can be registered directly. However, in case a camera is directed to a specular surface, not the surface itself but a distorted image of the surrounding scene is registered. Hence such methods are not suitable for the 3D-measurement of specular surfaces if artificial targets cannot be attached to the surfaces. Deflectometry, also known as shape from specular reflection, is an image-based method that registers reference structures via the specular surface of an object. Hereby the 3D reconstruction of surface points is based on the registered distortion of the reference structures. Such a reconstruction is subject to an ambiguity regarding the surface normals which must be resolved.

Petz and Tutsch (Petz and Tutsch, 2004) have proposed two deflectometric techniques to resolve this ambiguity. The first one, called passive raster photogrammetry, requires a motorized stage in order to move a reference grid to two different positions. The second one, called active raster photogrammetry, is making use of a second camera. Seßner and Häusler (Seßner and Häusler, 2004) proposed a deflectometric technique that makes use of a special optic. For the reconstruction of smooth specular surfaces the ambiguity can be resolved if the absolute coordinates of at least one surface point are known. Nevertheless even to get the absolute coordinates of a single point the ambiguity regarding its surface normal must be resolved. Hence, this would still require such additional or

special hardware components as stated above. Such hardware components increase the complexity and cost of deflectometric systems.

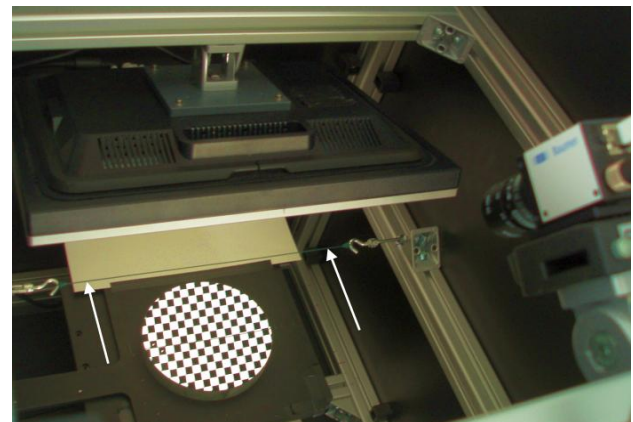


Figure 1. Measurement system with thin wire (white arrows). The LC display is shown from the back in the upper half. The camera at the right acquires the checkerboard image which is reflected on the round mirror.

Our goal is to keep complexity and costs of the 3D measurement system for smooth specular surfaces as low as possible. To achieve this we developed a new technique for measuring absolute points within a deflectometric measurement system. We use these absolute points as starting values for a region-growing algorithm in order to reconstruct the 3D surface

* Corresponding author.

of a specular object. Our method can be applied in a calibrated deflectometric measurement system consisting of a camera and a reference grid, shown on a LC display. The only hardware modification to such a system is to introduce a straight reference line w in object space, realized as a reference wire w that is forming a straight line in front of the reference grid (Figure 1).

2. METHOD

2.1 Measurement of absolute height values

Using a central projection imaging model, each image point together with the corresponding camera projection center defines the image ray r to the corresponding surface point P (Figure 3). For a specular surface the image ray r is reflected on the surface point P and the reflected ray r' intersects a reference grid at point P' . The intersection point P' can be determined by a coded fringe procedure (Reich, Ritter and Thesing, 1997). The height of the surface point P along the ray r still depends on the slope n of the surface. Different heights of P_i in combination with a slope n_i (as it is shown in Figure 2) can lead to the registration of the same intersection point P' . Hence, there exists an ambiguity between slope and height of a surface that must be resolved.

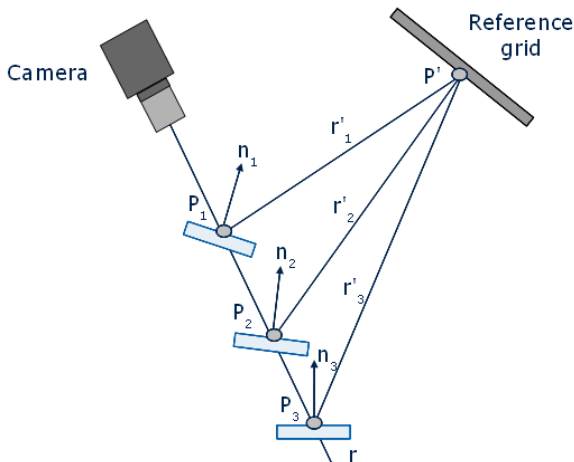


Figure 2. Ambiguity between slope and height

From Figure 3 it can be seen that this ambiguity can be resolved if an additional point P'' is known along the reflected ray r' .

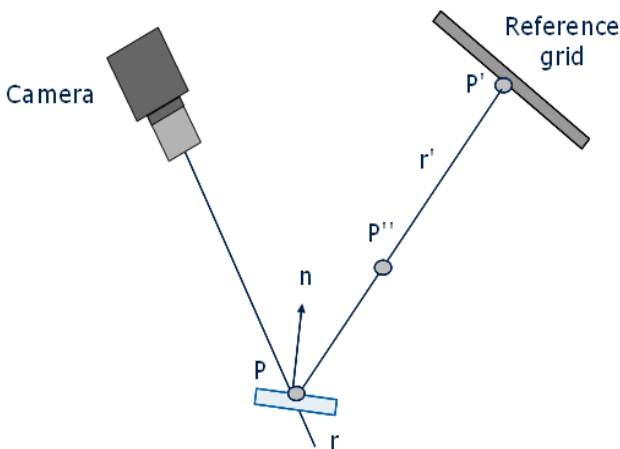


Figure 3. Resolving the ambiguity with a point in space

The reflected ray r' lies in a plane E defined by the image ray r and the intersection point P' . If we know a line w that intersects with the reflected camera ray we can compute a point P'' on the reflected camera ray by intersecting the line w with the plane E . Hence, we can already perform the triangulation even if we only know that the reflected camera ray intersects a given line (Figure 4).

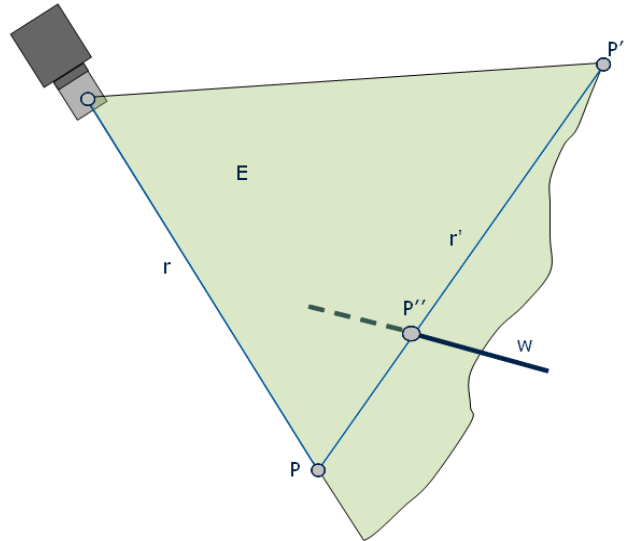


Figure 4. Resolving the ambiguity from Figure 2 by using a line in space

Furthermore, we can define a plane E' that is defined by the point P' and the line w . If a reflected ray r' intersects the line w and we know its intersection point P'' then we can also compute the plane E' . Since the reflected ray r' must lie within this plane we can compute its reflection point P by intersecting the plane E' with the camera ray r (Figure 5).

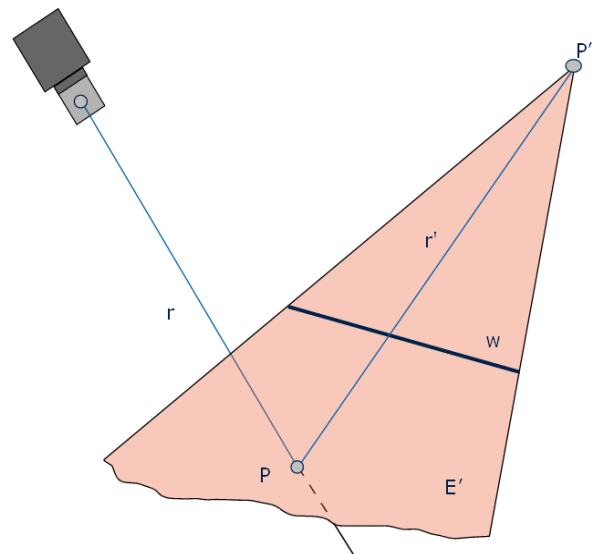


Figure 5. Intersection between camera ray and plane

In order to constrain the triangulation the line w must not lie within the plane E (Figure 5). For each reflected ray we must determine, to which one of the following classes it belongs:

- Reflected ray intersects wire and reference grid (Figure 6 and Figure 7)
- Reflected ray intersects only reference grid (Figure 8a)
- Reflected ray intersects only wire (Figure 8b)

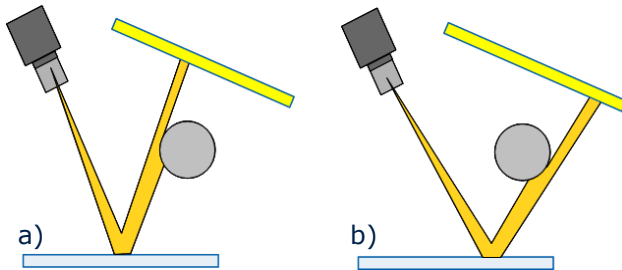


Figure 6. Schematic model for a reflected ray that intersects the wire and the reference grid. Note that this is a model where the wire is thicker than the reflected ray.

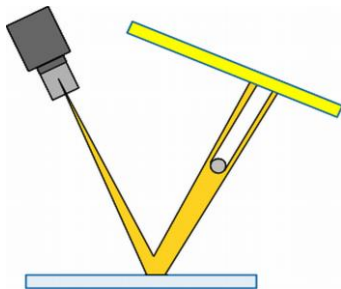


Figure 7. Schematic model for a reflected ray that intersects the wire and the reference grid. Note that this is a model where the wire is thinner than the reflected ray.

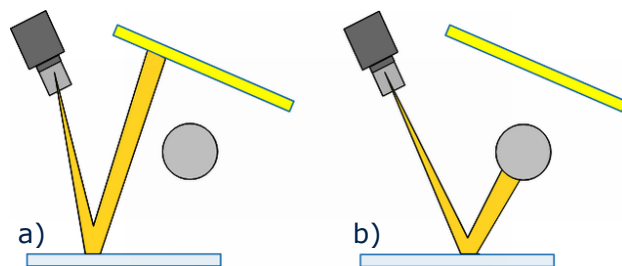


Figure 8. (a): Schematic model for a reflected ray that intersects only the reference grid. (b): Schematic model for a reflected ray that intersects only the wire.

We can do this classification based on the image intensity of the camera pixel that is related to the camera ray. For the acquisition of such a camera image a white image is displayed on the reference grid (i.e. shown on the LC display).

An enlargement of a camera image is shown in Figure 9. This image contains a mirrored view of a section of the wire. Hence, from this image we can do the classification for the reflected rays. Rays belonging to the class “Reflected ray intersects wire and reference grid” (Figure 6) can be identified based on pixels having medium grey values. In Figure 9, some of those pixels

are marked with a blue dot. Rays belonging to the class “Reflected ray intersects only reference grid” (Figure 8a) can be identified based on pixels having bright grey values. Rays belonging to the class “Reflected ray intersects only wire” (Figure 8b) can be identified based on pixels having dark grey values.

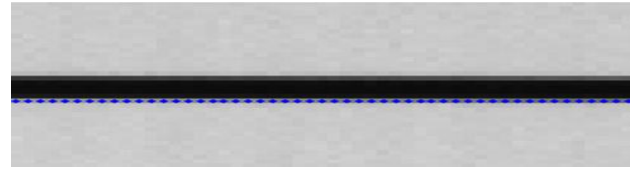


Figure 9. Enlargement of a camera image showing a mirrored view of a section of the wire.

For the rays belonging to the classes “Reflected ray intersects wire and reference grid” (Figure 6) and “Reflected ray intersects only reference grid” (Figure 8a) the intersection point P' can be determined by a coded fringe procedure.

For the rays belonging to the class “Reflected ray intersects only wire” (Figure 8b) no intersection point P' can be determined. Hence, they neither contribute to the determination of starting points, nor can they be used for the region-growing approach itself. During the region-growing an extrapolation routine will be applied in order to handle all rays belonging to this class.

When the wire is thicker than the reflected ray (Figure 6) it should be differentiated whether the reflected ray intersects the wire on the front side or on the back side. In that case two parallel lines w_1 and w_2 can be used (to model the border of the wire) instead of one line w . The distance between these two lines must be equal to the diameter of the wire. In this case the class “Reflected ray intersects wire and reference grid” should be split into the classes “Reflected ray intersects wire at front side and reference grid” (Figure 6a) and “Reflected ray intersects wire at back side and reference grid” (Figure 6b).

When the wire is thinner than the reflected ray (Figure 7) the wire can be modelled as a single line w .

2.2 Theoretical accuracy analysis

This accuracy analysis is for an ideal deflectometry system with perfect calibration. It should show how the accuracy of the triangulation of absolute surface points depends on the accuracy of the detection of point P'' .

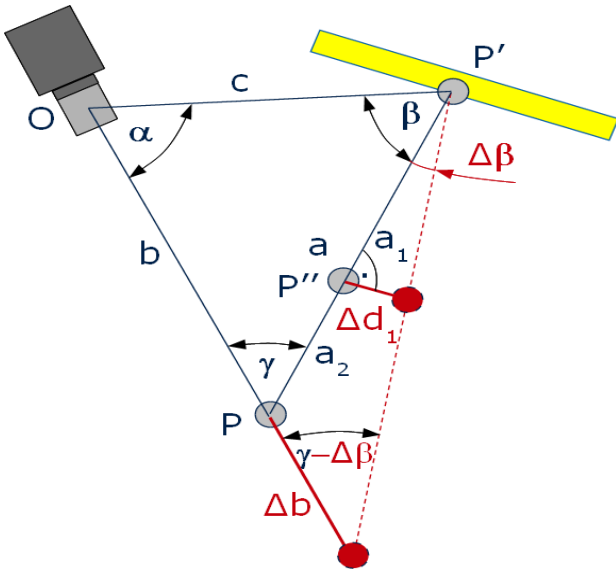


Figure 10. Model for the theoretical accuracy analysis

In Figure 10 the underlying model for this accuracy analysis is shown. We simulate an error in the position of the point P'' . The direction of the position error is perpendicular to the reflected ray.

$$\Delta\beta = \arctan\left(\frac{\Delta d_1}{a_1}\right) \quad (1)$$

$$\frac{\sin(\gamma - \Delta\beta)}{a} = \frac{\sin(\Delta\beta)}{\Delta b} \quad (2)$$

from (2) we obtain

$$\Delta b = a \frac{\sin(\Delta\beta)}{\sin(\gamma - \Delta\beta)} \quad (3)$$

where $\Delta\beta$ = angle error
 Δd_1 = position error of point P''
 a_1 = distance between point P' and point P''
 a = distance between camera projection center and point P
 γ = angle between camera ray and reflected ray
 Δb = resulting distance error along the camera ray

2.3 Calibration

The goal of the calibration is to recover the intrinsic camera parameters and the location and orientation of the camera, the reference grid and the wire relative to a common object coordinate system.

Camera calibration

The camera is calibrated by estimation of the intrinsic (focal length, principal point and distortion) and extrinsic camera parameters. These parameters can be estimated with Bouquet's camera calibration toolbox (Bouquet). For the extrinsic camera calibration procedure a checkerboard calibration pattern is placed on the chuck in the location of the object to measure

(Figure 11). The location of this calibration pattern defines the object coordinate system.

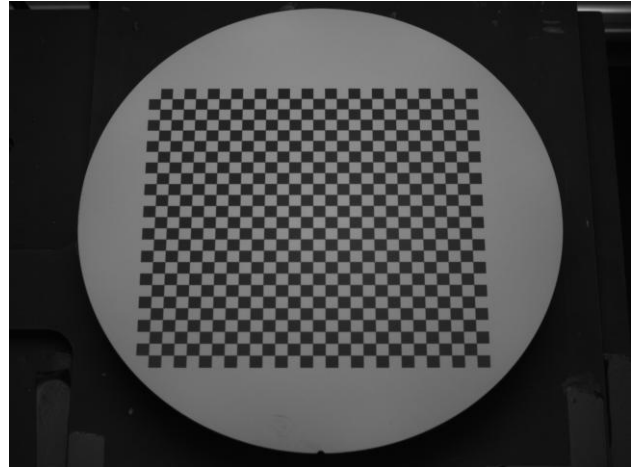


Figure 11. Camera image of the calibration target.

Reference grid calibration

The location and orientation of the reference grid within the object coordinate system can be estimated with the calibrated camera. For this estimation a flat first surface mirror is placed on the chuck and a checkerboard calibration pattern is displayed on the reference grid. The top surface of this mirror must be exactly at the plane $z=0$ (which has already been defined by the external camera calibration). The camera observes the reflection of the checkerboard image in the mirror (Figure 12).

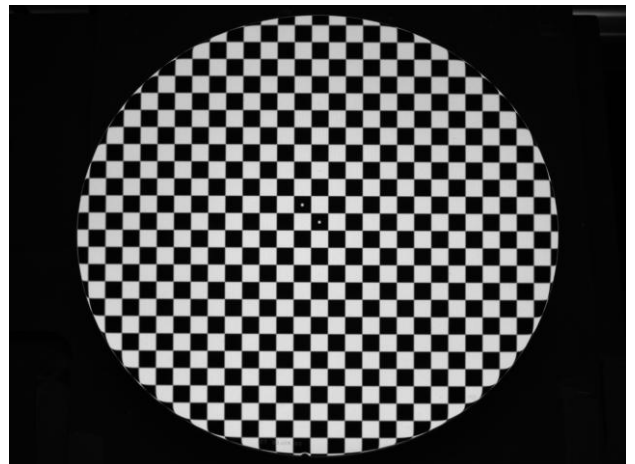


Figure 12. Camera image of the reflection of the calibration pattern displayed on the reference grid.

Based on this camera image and the known size of the displayed checkerboard, the location and orientation of the reference grid can be estimated with Bouquet's camera calibration toolbox (Bouquet). Thereby it must be taken into account that the reference grid has been mirrored at the plane $z=0$. From Figure 12 it can be seen that two conjoined black squares are both marked with a white dot. This allows the identification of the center of the checkerboard image within the camera image, which is necessary for this calibration.

Wire calibration

The location and orientation of the wire within the object coordinate system can be estimated with the calibrated camera. For this estimation a first surface mirror is placed on the chuck and a white image is displayed on the reference grid (i.e. shown on the LC display). The top surface of this mirror must be exactly aligned with the plane $z=0$ (which has already been defined by the external camera calibration). In practice this can be achieved best, when both the calibration target and the first surface mirror have the same thickness. Such a setup is shown in Figure 13. The camera observes the wire and the reflection of the wire in the mirror. A camera image from the wire calibration process is shown in Figure 14.

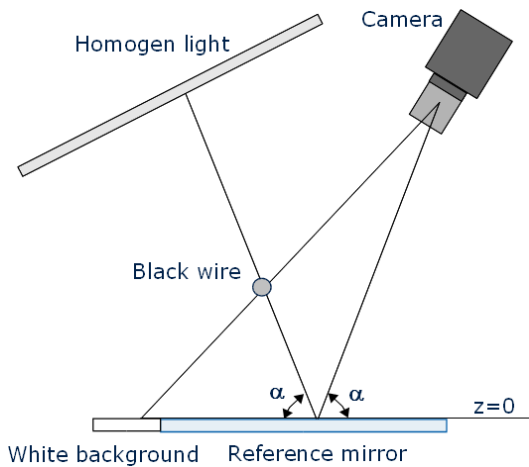


Figure 13. Direct and mirrored observation of the wire by the camera



Figure 14. Camera image from the wire calibration process

In Figure 15 the underlying model for the wire calibration is shown. The line w is modelled with a straight line in space. Since this line is reflected in a flat mirror, its reflection must also take place along a straight line in space. Since the top surface of the mirror is located at $z = 0$ the z -coordinates of the reflected line points are all zero. We can transform the points where the reflection takes place to the object coordinate system and fit a line to these points. With this line and the camera projection center O' we can define the plane $E3$ in object space. By setting the z -coordinate of the camera projection center to its negative value we can define the plane $E4$ in object space.

We can also determine the location of the points that belong to the wire and are projected to $z = 0$ along the camera rays. We can fit a line to these projected points. With this line and the camera projection center O' we can define the plane $E2$ in object space. The intersection between plane $E2$ and $E4$ defines a line in space w that defines the location of the wire.

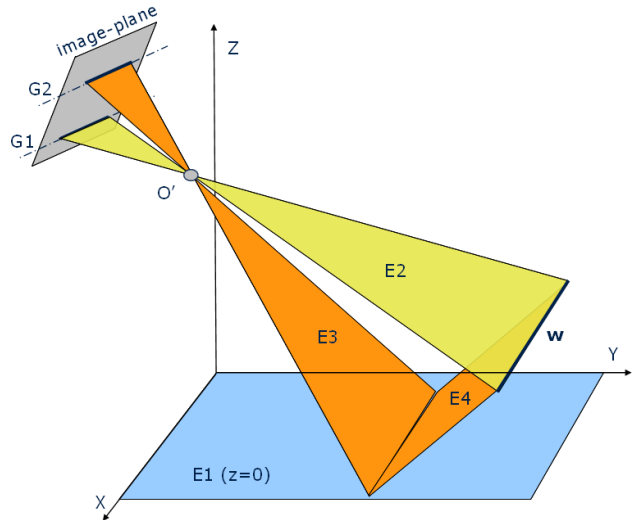


Figure 15. Model for the wire calibration

A detail from the calibration image, showing a mirrored view of a part from the wire is shown in Figure 16. An sub-pixel accuracy edge detection algorithm (Steger, 1998) can be applied to detect the reflection of the wire within the image.

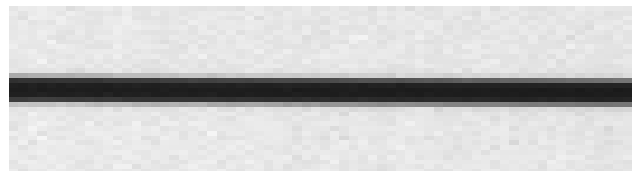


Figure 16. Enlargement of the calibration image, showing a mirrored view of part of the wire.

A detail from the calibration image, showing a direct view of a part from the wire is shown in Figure 17. An sub-pixel accuracy edge detection algorithm (Steger, 1998) can be applied to detect the wire within the image.



Figure 17. Detail from the calibration image, showing a direct view of part of the wire.

3. RESULTS

The hardware of the measurement system is composed of a Baumer TXG 13 CCD-camera, a 16 mm Pentax C1416-M lens and a 19-inch HP LP1965 flat panel monitor.

In order to determine how the accuracy of a triangulated starting point affects the overall accuracy of the surface reconstructed from deflectometric measurement data, we carried out measurements on a reference object. A concave spherical reference mirror with a specified radius of curvature of 3048 mm and a diameter of 152 mm has been used as a reference object.

In order to show the problems that can appear when a starting point is just guessed, but not measured we first reconstructed the surface of the reference object, based on a poorly estimated starting point. Therefore a height offset of 1.7 mm was added to the real starting point. The reconstruction result that is based on the poorly estimated starting point is shown in Figure 18.

For an accurate reconstruction we measured the absolute coordinates of one surface point with the proposed triangulation method. Then we reconstructed the surface of the reference object by using these coordinates as a starting point for the reconstruction algorithm. The reconstruction that is based on an accurate measured starting point is shown in Figure 19.

For the region-growing based reconstruction the height values at the areas of the reflection of the wire could successfully be extrapolated from the neighbouring areas.

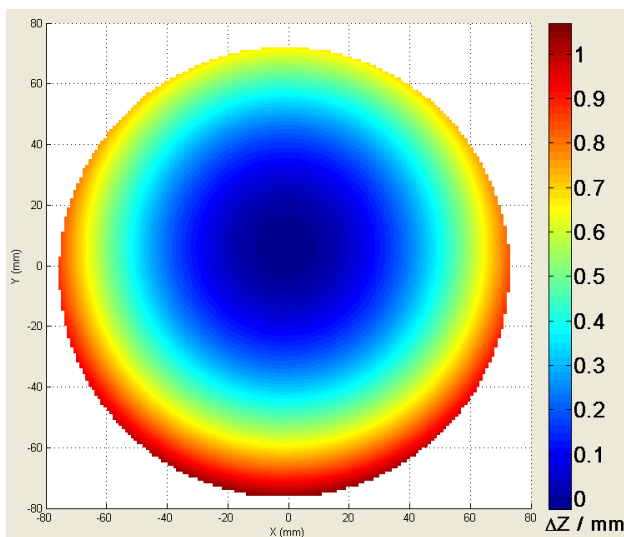


Figure 18. Shape of the spherical mirror, reconstructed based on deflectometric measurement data and on the absolute coordinates of one surface point that was estimated with a height offset of 1.7 mm (i.e. without measuring a starting point).

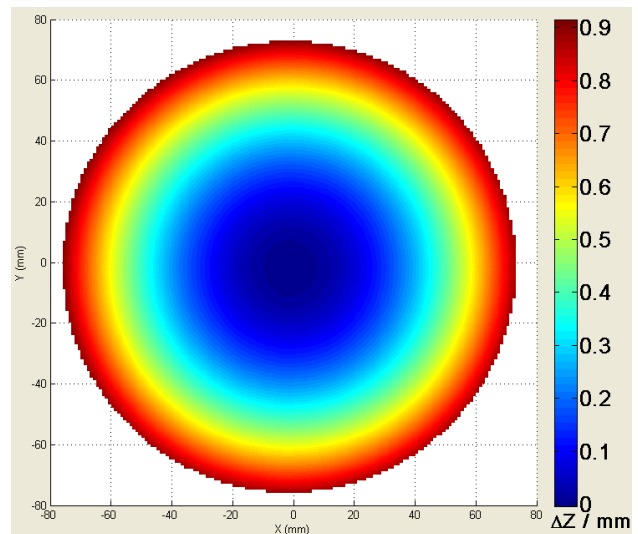


Figure 19. Shape of the spherical mirror, reconstructed based on deflectometric measurement data and on the absolute coordinates of one surface point that has been measured with the proposed triangulation method.

4. CONCLUSION

This investigation demonstrated how the principle of optical triangulation can be adapted in order to measure the absolute coordinates of some points on a specular surface. We can show how such a triangulation method can be implemented within a deflectometric measurement system. We can apply this method in order to provide starting points that are required for a surface reconstruction method based on a region-growing approach.

REFERENCES

- Bouquet, J. B., "Camera Calibration Toolbox". http://www.vision.caltech.edu/bouquetj/calib_doc/. (accessed 10 Oct. 2008)
- Horbach, J., Dang, T., 2009. 3D reconstruction of specular surfaces using a calibrated projector-camera setup, *Machine Vision and Applications*, 21(3), pp. 331-340
- Petz, M., Tutsch, R., 2004. Rasterreflexions-Photogrammetrie zur Messung spiegelnder Oberflächen. *tm - Technisches Messen* 71, 7-8, pp. 389-397
- Reich, C., Ritter, R., Thesing, J., 1997. White light heterodyne principle for 3D-measurement. *Proceedings of SPIE Vol. 3100 - Sensors, Sensor Systems and Sensor Data Processing*, pp. 236-244.
- Seßner, R., Häusler, G., 2004. Richtungscodierte Deflektometrie (RCD). *DGaO-Proceedings*, Onlinezeitschrift der Deutschen Gesellschaft für angewandte Optik.
- Steger, C., 1998. An Unbiased Detector of Curvilinear Structures, *IEEE Transactions on Pattern Analysis and Machine Intelligence*, 20(2), pp. 113 - 125